Available online at BCREC website: https://bcrec.id

Bulletin of Chemical Reaction Engineering & Catalysis, 18 (4) 2023, 640-647

Research Article

Synthesis of W-Doped TiO_2 Material Ratio Using One-Step Solvothermal Method and Treatment Orientation of Volatile Organic Compounds

Hung Dung Chau[1,2], Tran Thi Tuu[1,2], Phung Chi Sy[2], Lam Van Tan[1,2], Thi Kim Ngan Tran[1,2,*]

[1]*Institute of Applied Technology and Sustainable Development, Nguyen Tat Thanh University, Ho Chi Minh City, Vietnam*

[2]*Faculty of Food and Environmental Engineering, Nguyen Tat Thanh University, Ho Chi Minh City 700000, Vietnam*

Received: 17th May 2023; Revised: 10th November 2023; Accepted: 11st November 2023
Available online: 14th November 2023; Published regularly: December 2023

Abstract

In TiO_2 photocatalysts have been interested in the world thanks to many advantages in handling toxic compounds, with great potential for practical application at low cost. However, the electron-hole recombination rate is still high and can not be processed under visible light, which is a major limitation of this material. Modification of TiO_2 by W^{6+} is a possible solution, however there is still little research and the optimal W^{6+} ratio in small amounts is still low. The material was synthesized by a one-stage solvothermal method at 200 ºC for 10 hours, without using any surfactants or post-reaction calcination with doped W molar ratios of 0.5%, 1%, and 1.5%. The result was that the TiW-1.5% catalyst sample had the highest specific surface area of 175 m^2/g, higher than pure TiO_2 of 160.0 m^2/g. The W^{6+} ion successfully replaced Ti^{4+} in the TiO_2 crystal lattice, reducing the band gap energy of the catalytic sample to 2.88 eV with the TiW-1.5% sample. For TiW-0%, the formaldehyde decomposition ability is 53.50%. Doping W into TiO_2 increased catalytic efficiency, with a material sample with an optimal modified W content of 1.5% mol W having a formaldehyde decomposition efficiency of 71.98%. Research results show that W modification can improve the activity of TiO_2 and increase the efficiency of volatile organic compound treatment .

Keywords: Volatile Organic Compounds; VOC; W-doped TiO2; solvothermal; formaldehyde

How to Cite: H. D. Chau, T. T. Tuu, P. C. Sy, L. V. Tan, T. K. N. Tran (2023). Synthesis of W-Doped TiO2 Material Ratio Using One-Step Solvothermal Method and Treatment Orientation of Volatile Organic Compounds. *Bulletin of Chemical Reaction Engineering & Catalysis*, 18(4), 640-647 (doi: 10.9767/bcrec.18198)

Permalink/DOI: https://doi.org/10.9767/bcrec.18198

1. Introduction

Volatile Organic Compounds (VOCs) are highly toxic and negatively affect human health. They can cause skin, eye and respiratory irritation, and even cancer when exposed for a prolonged period [1]. Many pharmaceutical and chemical industries consume organic solvents and therefore large amounts of VOCs are released into the environment. Currently, TiO_2 photocatalysts are attracting the attention of researchers due to many advantages, such as high catalytic activity, non-toxicity, and the ability to effectively treat pollutant compounds in water and air with high economic efficiency [2].

TiO_2-based photocatalysts have been profoundly studied for their benefits such as non-toxicity, high catalytic activity, cost-saving, etc. [3-5]. TiO_2 is a n-type semiconductor able to generate pairs of electrons and holes for photodegradation where oxygens and hydroxyls are

* Corresponding Author.
Email: nganttk@ntt.edu.vn (T.K.N.T.)

the main oxidants [6,7]. Application of these catalysts, however, still face challenges as TiO_2 possesses wide band gap preventing it from utilizing visible spectrum, and high rate of electron - hole recombination [8]. Many researches focus on overcoming these obstacles by doping other elements into TiO_2 lattice or composing it with other materials, in which introducing metals has been proven a facile and efficient method.

The valence band of TiO_2 consists mainly of O-2p states, while the conduction band is mainly Ti-3d. In order to reduce recombination, ions must create a new energy level between these regions. The ionic radius of W^{6+} (0.60Å) is approximately close to Ti^{4+}'s (0.605Å), which makes it easy to substitute into the lattice, and at the same time can create a new energy region below the conduction band [9-11]. The bandgap energy of WO_3 is 2.5 eV showing its potential to improve TiO_2 characteristics. Several authors have studied W-doped TiO_2 ability to decompose VOCs, but the amount of these researches are still modest when compared to that of other metals, such as Fe or Ni [12-14]. The metal in the TiO_2 crystal lattice greatly influences the trapping and electron transport to the catalyst surface. Choi *et al.* found that denaturation with Fe^{3+}, Mo^{5+}, Ru^{3+}, Os^{3+}, Re^{5+}, V^{4+}, and Rh^{3+} at 0.1 – 0.5 % significantly increased catalytic activity for both reduction and oxidation, however For each metal, the optimal ratio is different [15]. In order to solve the above problems, the goal of this thesis is to successfully synthesize W photocatalysts modified by TiO_2 based on the processes performed by other groups of authors, thereby orienting the application. materials into the experimental gas treatment system in the future.

2. Materials and Methods

2.1 Materials

All reagents in this study are commercial products, and used without further treatment. Titan(IV) chloride ($TiCl_4$ – 99.5%), and Tungsten(VI) chloride (WCl_6 – 99.9%) were purchased from Sigma Aldrich, USA. Ethanol absolute (C_2H_5OH, 99%), and acetone were produced by Merck, Belgium. Purified water was also employed.

2.2 Synthesis of low ratio W-doped TiO_2

W-modified TiO_2 material was prepared by a one-step thermal mixing method based on the research of Pham *et al.* [16]. First, an amount of salt m (g) (corresponding to WCl_6 molar ratios of 0.5%, 1%, and 1.5%) WCl_6 was completely dissolved in 50 mL of ethanol and stirred for 20 minutes on a stirring stove. From there, heat at 50 °C until the salt is completely dissolved in the ethanol. Put the solution in an ice bath to cool for 30 minutes, while continuing to stir on the induction cooker. Then, use a small micropipette of 0.550 mL $TiCl_4$. The resulting solution were placed in Teflon - covered by an autoclave. The hydrothermal reaction takes place at 200 °C for 10 hours. The suspension after the reaction was centrifuged and washed several times with distilled water (4 -5 times). The solid was dried at 80 °C for 24 hours and then finely ground to obtain W-modified TiO_2 catalyst material.

2.3 Characterizations

The material was evaluated for structural characterization based on a number of analytical methods such as crystal structure determined by X-ray diffraction (XRD) on a D8-advance device (Bruker, Germany) at 2θ 10 conditions. - 70 degrees, stop angle 0.03 degrees, dwell time 0.7 seconds/degree. The surface of the material is shown in SEM images taken by JEOL's S4800 (Japan). The TEM method was analyzed on Jeol's JEM 2100, measured at 200 kV, the TEM resolution can provide information and the size and shape of the material. BET (Brunauer-Emmett-Teller) surface area measurement method was performed on Micromeritics 2020 equipment of Micromeritics (USA), measuring parameters of isothermal absorption - desorption, pore size, pore volume and hole structure. The light absorption of the catalyst was characterized by UV-Vis-DRS method on a Shizumazdu 2600 device, room temperature, at songd 350 – 750 nm. The composition and elements of the materials were analyzed on VietSpace 5006-HQ02 instrument, Amptex USA.

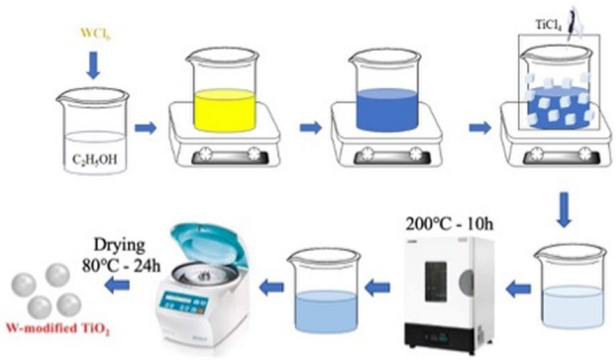

Figure 1. Illustrate the synthesis of W doped TiO_2

3. Results and Discussion

3.1 Structural Characteristics

XRD spectra of TiO_2 and W-modified TiO_2 catalyst samples with different ratios are shown in Figure 2. The XRD spectrum shows that diffraction peaks were recorded at positions 25.3º, 37.8º, 48.0º, 53.9º, 55.1º, and 62.8º, corresponding to the (101), (004), (200), (105), (211), and (204), respectively, showing the orientation of Anatase TiO_2 phase formation (JCPDS – 84 – 1286). Because the color of the composite material changes, but the phase structure does not change, it can be predicted that W has been incorporated into the structure of TiO_2 and there is no formation of WO_3/TiO_2 composite due to lack of emission. shows the characteristic diffraction peaks of WO_3 (JCPDS-20-1324) (at 2θ ~ 23.0º, 23.7º, 24.0º). There is not much difference in the peak position of the modified TiO_2 material samples compared to TiO_2. This may be due to the negligible difference in radius between W^{6+} (0.600 Å) and Ti^{4+} (0.605 Å), and the doping percentage is not much. No diffraction peaks of Rutile were detected, possibly due to the synthesis conditions of 200 ºC for 10 hours. Under this condition, amorphous TiO_2 is completely converted to anatase, but not enough to convert anatase to the rutile phase [17]. Comparing between W-modified TiO_2 samples, as the doping W content increases, the signal intensity decreases and the peak width increases. This shows that W-modified TiO_2 has reduced the crystal size.

Figures 3 the structure, morphology of the composites, and grain size at different coefficients, respectively. TEM analysis results of 4 samples show that all samples contain single crystalline particles and all have a spherical shape typical of the anatase phase. The particle size of TiW-0% ranges from 10 to 16 nm. W-modified TiO_2 samples have smaller sizes, specifically TiW-0.5% is 8-13 nm, TiW-1% is 7 - 11 nm, and TiW-1.5% is mainly 6 – 10 nm. The grain size matches the crystal size obtained from the XRD spectrum.

Figure 4 and Table 1 show the distribution of elements of O, Ti, and W in the material. It can be seen that compared to Ti and O, which are uniformly distributed, W is less evenly distributed. This may also be the reason why the %W ratio in the material sample when surveyed is quite different from the theoretical calculation [18]. The elemental composition of W and Ti in the W-modified TiO_2 samples at the ratios is shown in Table 2. Errors compared with theory are still large, possibly caused by $TiCl_4$ hydrolysis to solid TiO_2 before W^{6+} can be substituted into the crystal lattice (Equation (3)). On the other hand, the interaction between the reaction factors, solvent concentration, pH, and $TiCl_4$ solution addition rate has not been investigated and controlled.

$$TiCl_4 + H_2O \rightarrow TiO_2 + HCl \quad (3)$$

N_2 adsorption and desorption methods help determine the specific surface area and pore size of the material. The analysis results are calculated according to the BET equation and are presented in Table 3. The specific surface area of the material increases with increasing W doping amount and is highest at 175.5 m^2/g in the sample with a 1.5% W ratio. This is also consistent with previous XRD and TEM results. The material has an anatase structure,

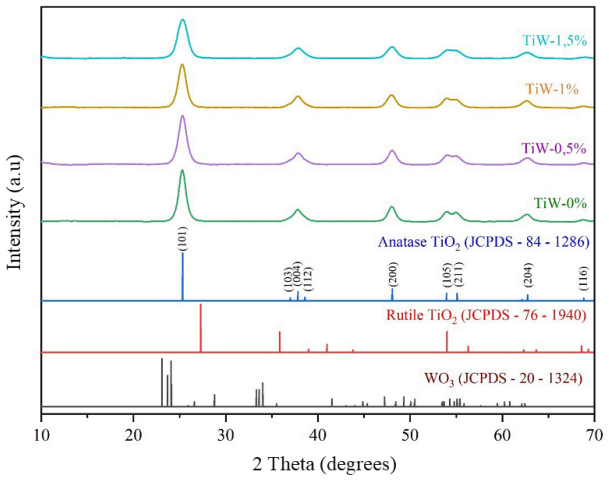

Figure 2. XRD pattern of W doped TiO_2 at different scales

Table 1. Elemental ratio by EDS in W-modified TiO_2 catalyst sample (Table 1 is not cited in text). What is difference between Table 1 and 2)

Sample	%mol W
TiW-0.5%	1.0
TiW-1.0%	1.6
TiW-1.5%	2.8

Table 2. Elemental ratio by XRF in W-modified TiO_2 catalyst sample

Sample	%mol W
TiW-0.5%	0.4
TiW-1.0%	1.3
TiW-1.5%	1.5

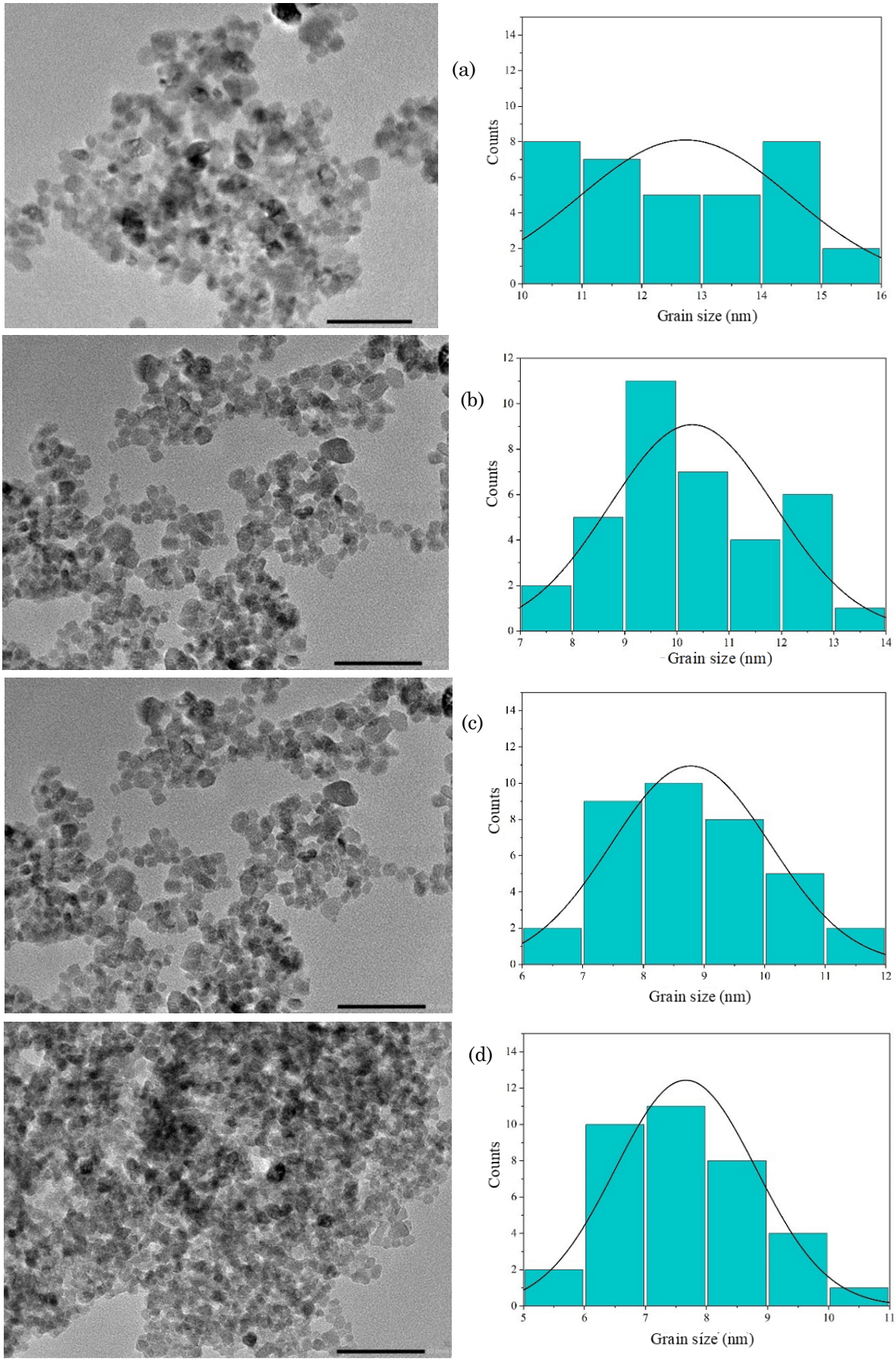

Figure 3. TEM images of W doped TiO_2 at different scales a) (a) TiW-0%, (b) TiW-0.5%, (c) TiW-1%, (d) TiW-1.5%

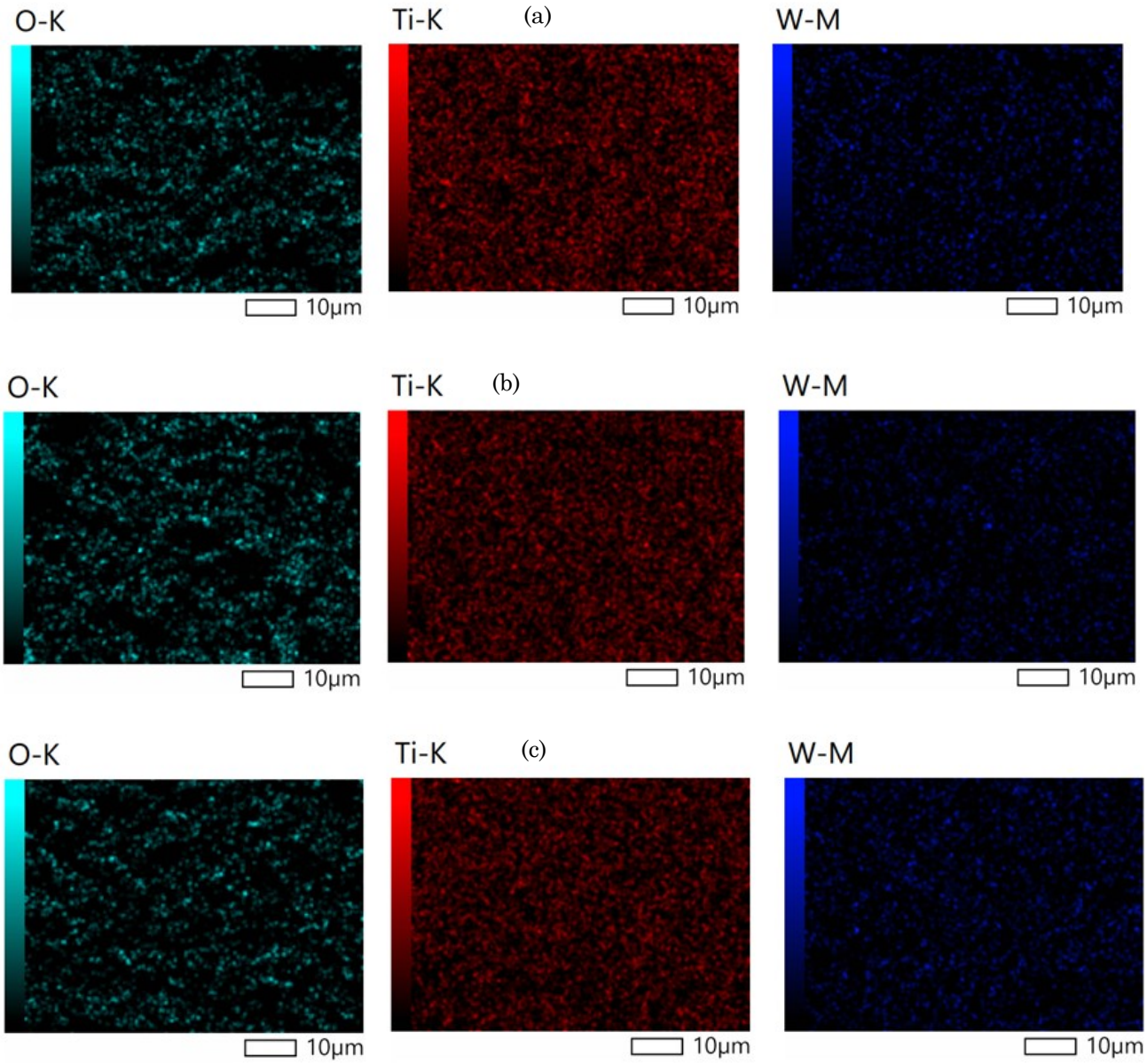

Figure 4. Distribution mapping of elements in the material (a) TiW-0.5% (b) TiW-1%, (c) TiW-1.5%

Table 3. Specific surface area and pore size of catalyst samples

Sample	Specific surface area (m^2/g)	Pore size (nm)
TiW-0%	160.0	5.5
TiW-0.5%	164.6	5.5
TiW-1%	168.6	4.9
TiW-1.5%	175.5	4.6

so the particle size is smaller, leading to a larger specific surface area. The reason for the large specific surface area of the synthesized material may be due to the one-stage solvothermal synthesis process that does not use structure-directing agents, and the precursors used are inorganic substances, thus avoiding the influence of organic macromolecules and there is no post-reaction heat treatment stage.

UV-Vis DRS diffuse reflectance spectroscopy method was used to determine the optical properties of W-doped TiO_2 materials. Figure 5 shows the band gap energy of TiO_2 and W-modified TiO_2 catalyst samples with different ratio. The synthesized TiO_2 sample has a band gap energy level of 3.02 eV, lower than anatase TiO_2 of 3.20 eV. The explanation for this may be because the particle size has been significantly reduced when synthesized by the one-stage solvothermal method [19,20]. W-modified TiO_2 samples have a reduced band gap energy compared to TiO_2, expanding the visible light absorption region, larger than 420 nm. This decrease in band gap energy can be due to the formation of oxygen vacancies, as a result of the

doping process. W substitution into the TiO_2 lattice can generate many oxygen vacancies, creating a small band below the conduction band of the TiO_2 photocatalyst [21].

3.2 Orientation for Handling VOCs (Formaldehyde)

Table 4 and Figure 6 show the formaldehyde concentration in the gas sample before and after going through the gas treatment system and when using W-modified TiO_2 catalyst with different W ratios and the treatment efficiency of the samples. catalysis. Investigation reaction with formaldehyde sample drop volume of 0.05 mL and 0.024 mL of distilled water corresponding to 70% humidity, air flow through the catalyst is 300 mL/min and collected for 10 minutes to fill the bag gas. After the experiment, the air bag was subjected to gas chromatography analysis to determine formaldehyde concentration. The formaldehyde concentrations in the airbag samples corresponding to the catalyst samples TiW-0%, TiW-0.5%, TiW-1%, and TiW-1.5% are 73.0 mg/m^3, 63.0 mg/m^3, 57.5 mg/m^3, and 44.0 mg/m^3, with formaldehyde removal efficiency of 53.50%, 59.87%, 63.38%, and 71.98%, respectively. It can be seen that the formaldehyde decomposition ability of TiW-0% catalytic material is not high. When using W-modified TiO_2 catalyst, the treatment efficiency increased with the highest TiW-1.5% sample being 71.98%. This may indicate that W doping helps increase the catalytic activity of the material.

Table 4. Preliminary survey on the possibility of treating formaldehyde with W-modified TiO_2

Sample	Initial formaldehyde concentration (mg/m^3)	Formaldehyde concentration after reaction C_m (mg/m^3)	Efficiency (%)
TiW-0%	157.0	73.0	53.50
TiW-0.5%		63.0	59.87
TiW-1%		57.5	63.38
TiW-1.5%		44.0	71.98

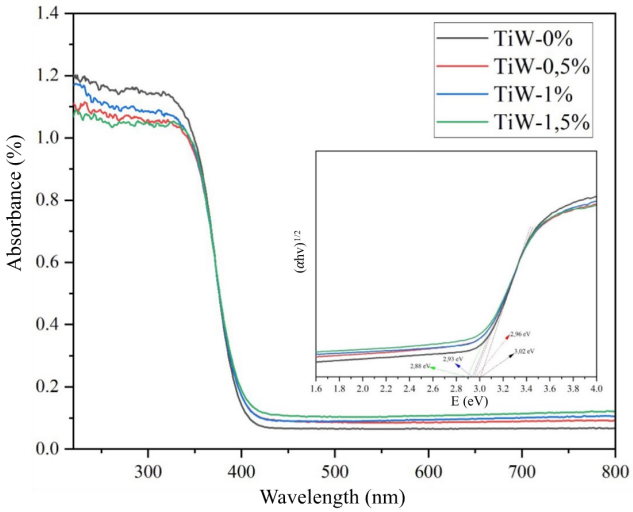

Figure 5. UV-Vis-DRS of W-modified TiO_2 samples

4. Conclusions

W-modified TiO_2 material was successfully synthesized using a one-stage solvothermal method at 200 °C for 10 hours, without using any surfactants or a calcination stage after reacting with different molar ratios. W doping were varied 0.5%, 1%, and 1.5%. W-modified TiO_2 material through XRD spectrum was determined to have an anatase phase crystal structure, without the appearance of the WO_3 peak. The presence of W in the material is proven from the XRF spectrum with a ratio close to the theoretical calculation. TEM images show that W-modified TiO_2 has a spherical shape, smaller particle size and more uniform distribution than TiO_2, with the smallest size of the TiW-1.5% sample in the range of 6 - 10 nm. The specific surface area of the particles was determined by N_2 adsorption and desorption combined with the BET theoretical equation. The result was that the TiW-1.5% catalyst sample had the highest specific surface area of 175 m^2/g, higher than pure TiO_2 of 160.0 m^2/g. The W^{6+} ion successfully replaced Ti^{4+} in the TiO_2 crystal lattice, reducing the band gap energy of the catalytic sample to 2.88 eV with the TiW-1.5% sample. From there, it is possible to expand research based on TiW-1.5% material to improve photocatalytic ability in the visible light region to treat gas samples contaminated with toxic organic vapors.

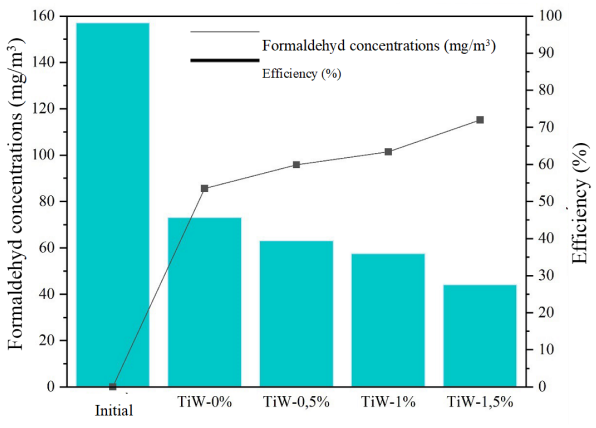

Figure 6. Effect of W-modified TiO_2 ratio on formaldehyde treatment efficiency

.Acknowledgments

This study was supported by grants from Nguyen Tat Thanh University, Ho Chi Minh City, Viet Nam.

CRediT Author Statement

Author Contributions: *H.D. Chau*: Conceptualization, Methodology, Investigation, Resources, Data Curation; *T.T. Tu*u: Visualization, Software, Project Administration; *T.K.N. Tran*: Writing, Review and Editing, Writing Draft Preparation, Writing, Review and Editing; *L.V. Tan*: Investigation, Resources, Writing, Review and Editing, Validation. All authors have read and agreed to the published version of the manuscript.

References

[1] Antonelli, M., Donelli, D., Barbieri, G., Valussi, M., Maggini, V., Firenzuoli, F. (2020). Forest volatile organic compounds and their effects on human health: A state-of-the-art review. *International Journal of Environmental Research and Public Health*, 17(18), 6506. DOI: 10.3390/ijerph17186506

[2] Stephen, L. (2020). *Titanium dioxide versatile solid crystalline: An overview*. Intech Open.

[3] Mergenbayeva, S., Kumarov, A., Atabaev, T. Sh., Hapeshi, E., Vakros, J., Mantzavinos, D., Poulopoulos, S. G. (2022). Degradation of 4-Tert-Butylphenol in Water Using Mono-Doped (M1: Mo, W) and Co-Doped (M2-M1: Cu, Co, Zn) Titania Catalysts. *Nanomaterials*, 12(14), 2326. DOI: 10.3390/nano12142326

[4] Ozimek, M., Palewicz, M., Hreniak, A. (2016). Optical Properties of TiO_2 Nanopowder Doped by Silver (Copper) during Synthesis or PVD Method. *Acta Physica Polonica A*, 129 (6), 1214–1219. DOI: 10.12693/APhysPolA.129.1214

[5] Thambiliyagodage, C., Mirihana, S. (2021). Photocatalytic activity of Fe and Cu co-doped TiO_2 nanoparticles under visible light. *Journal of Sol-Gel Science and Technology*, 99 (1), 109–121. DOI: 10.1007/s10971-021-05556-4

[6] Guo, Z., Wu, H., Li, M., Tang, T., Wen, J., Li, X. (2020). Phosphorus-doped graphene quantum dots loaded on TiO_2 for enhanced photodegradation. *Applied Surface Science*, 526, 146724. DOI: 10.1016/j.apsusc.2020.146724

[7] Senthilvelan, S., Chandraboss, V.L., Karthikeyan, B., Natanapatham, L., Murugavelu, M. (2013). TiO_2, ZnO and nanobimetallic silica catalyzed photodegradation of methyl green. *Materials Science in Semiconductor Processing*, 16 (1), 185–192. DOI: 10.1016/j.mssp.2012.04.018

[8] Humayun, M., Raziq, F., Khan, A., Luo, W. (2018). Modification strategies of TiO_2 for potential applications in photocatalysis: A critical review. *Green Chemistry Letters and Reviews*, 11 (2), 86–102. DOI: 10.1080/17518253.2018.1440324

[9] Ullah, I., Haider, A., Khalid, N., Ali, S., Ahmed, S., Khan, Y., Ahmed, N., Zubair, M. (2018). Tuning the band gap of TiO_2 by tungsten doping for efficient UV and visible photodegradation of Congo red dye. *Spectrochimica Acta Part A: Molecular and Biomolecular Spectroscopy*, 204, 150–157. DOI: 10.1016/j.saa.2018.06.046

[10] Teh, C. M., Mohamed, A.R. (2011). Roles of titanium dioxide and ion-doped titanium dioxide on photocatalytic degradation of organic pollutants (phenolic compounds and dyes) in aqueous solutions: A review. *Journal of Alloys and Compounds*, 509 (5), 1648–1660. DOI: 10.1016/j.jallcom.2010.10.181

[11] Filippatos, P.-P., Kelaidis, N., Vasilopoulou, M., Davazoglou, D., Chroneos, A. (2021). Structural, Electronic, and Optical Properties of Group 6 Doped Anatase TiO_2: A Theoretical Approach. *Applied Sciences*, 11(4), 1657. DOI: 10.3390/app11041657

[12] Mayoufi, A., Faouzi Nsib, M., Houas, A. (2014). Doping level effect on visible-light irradiation W-doped TiO_2–anatase photocatalysts for Congo red photodegradation. *Comptes. Rendus. Chimie*, 17(7–8), 818–823. DOI: 10.1016/j.crci.2014.01.019

[13] Santos, E., Catto, A.C., Peterline, A.F., Avansi Jr, W. (2022). Transition metal (Nb and W) doped TiO2 nanostructures: The role of metal doping in their photocatalytic activity and ozone gas-sensing performance. *Applied Surface Science*, 579, 152146. DOI: 10.1016/j.apsusc.2021.152146

[14] Sathasivam, S., Bhachu, D.S., Lu, Y., Chadwick, N., Althabaiti, S.A., Alyoubi, A.O., Basahel, S.N., Carmalt, C.J., Parkin, I.P. (2015). Tungsten Doped TiO_2 with Enhanced Photocatalytic and Optoelectrical Properties via Aerosol Assisted Chemical Vapor Deposition. *Scientific* Reports, 5(1), 10952. DOI: 10.1038/srep10952

[15] Choi, W., Termin, A., Hoffmann, M. R. (1994). The Role of Metal Ion Dopants in Quantum-Sized TiO_2: Correlation between Photoreactivity and Charge Carrier Recombination Dynamics. *The Journal of Physical Ch*emistry, 98 (51), 13669–13679. DOI: 10.1021/j100102a038

[16] Pham, H.Q., Huynh, T.T., Bach, L.G., Ho, V.T.T. (2021). Synthesis and characterization the multifunctional nanostructures $Ti_xW_{1-x}O_2$ (x = 0.5; 0.6; 0.7; 0.8) supports as robust non-carbon support for Pt nanoparticles for direct ethanol fuel cells. *International Journal of Hydrogen Energy*, 46(48), 24877–24890. DOI: 10.1016/j.ijhydene.2020.03.066

[17] Liao, Y. , Que, W. , Jia, Q. , He, Y. , Zhang, J. , Zhong, P. (2012). Controllable synthesis of brookite/anatase/rutile TiO_2 nanocomposites and single-crystalline rutile nanorods array. *Journal of Materials Chemistry*, 22, 7937–7944. DOI: 10.1039/c2jm16628c.

[18] Maira, A.J. , Yeung, K.L. , Lee, C.Y. , Yue, P.L. , Chan, C.K. (2000). Size Effects in Gas-Phase Photo-oxidation of Trichloroethylene Using Nanometer-Sized TiO_2 Catalysts. *Journal of Catalysis*, 192, 185–196. DOI: 10.1006/jcat.2000.2838.

[19] Jung, K.Y. Park, S.B. (2001). Effect of calcination temperature and addition of silica, zirconia, alumina on the photocatalytic activity of titania. *Korean Journal of Chemical Engineering*, 18, 879–888. DOI: 10.1007/BF02705612.

[20] Ho, V.T.T. , Chau, D.H. , Bui, K.Q. , Nguyen, N.T.T. , Tran, T.K.N. , Bach, L.G. , Truong, S.N. (2022). A High-Performing Nanostructured Ir Doped-TiO_2 for Efficient Photocatalytic Degradation of Gaseous Toluene. *Inorganics*, 10, 29. DOI: 10.3390/inorganics10030029.

[21] Komatani, S. , Aoyama, T. , Nakazawa, T. , Tsuji, K. (2013). Comparison of SEM-EDS, Micro-XRF and Confocal Micro-XRF for Electric Device Analysis. *e-Journal of Surface Science and Nanotechnology*, 11, 133–137. DOI: 10.1380/ejssnt.2013.133.